Original article
UDC 621.01
DOI 10.17073/0368-0797-2022-12-879-886
https://fermet.misis.ru/jour/article/view/2453

Strain and fracture of Cr – Mn – C – N steel in cast state

E. E. Deryugin, N. A. Narkevich, Yu. F. Gomorova

Institute of Strength Physics and Materials Science, Siberian Branch of the Russian Academy of Sciences (2/4 Akademicheskii Ave., Tomsk 634055, Russian Federation)

Abstract. The paper studies the influence of boundary conditions and the loading rate on the strain behavior and fracture of Cr–Mn–C–N austenitic steel in the cast state without additional heat treatment. Regularities of steel strain and fracture were analyzed on the basis of three-point bending test data of square-section samples with and without a notch, placed with a rib on supports. In addition to the initial stage of the steel elastic strain, this unconventional arrangement of the sample on supports enabled the detection of two more stages of strain development under the effect of an external applied force: the stage of nonlinear strain and the stage of discontinuous strain preceding the moment of sample failure. As the loading rate increases, it was demonstrated that the fracture resistance and the extent of the nonlinear strain stage of the sample with a notch decreases, and the extent of the discontinuous strain stage increases. The sample without a notch has a prolonged nonlinear strain stage and exhibits maximum strength in the absence of the discontinuous stage. The end of the nonlinear strain stage corresponds to the moment of sample failure. A characteristic property of cast steel under the given loading conditions is that the fracture of the sample is brittle, despite the prolonged stage of non-linear strain. Structural metallographic and diffractometric studies have shown that in all tests the steel fracture is brittle with-out traces of plastic yield. The nonlinear strain stage of steel is determined not by dislocation plastic yield, but by the mechanism of $\gamma \rightarrow \alpha'$ transformation in austenitic interlayers between nitride and carbide particles under the effect of an external applied force. The discontinuous strain stage of steel is associated with the process of stable crack propagation across the sample.

Keywords: cast Cr – Mn – C – N steel, dendritic structure, discontinuous decay, nitrides, bending test, fracture

Funding: The work was performed within the framework of the state task of the Institute of Strength Physics and Materials Science, Siberian Branch of the Russian Academy of Sciences, project FWRW-2021-0009 and supported by the Russian Science Foundation, grant RSF 22-29-00438.

For citation: Deryugin E.E., Narkevich N.A., Gomorova Yu.F. Strain and fracture of Cr–Mn–C–N steel in cast state. *Izvestiya. Ferrous Metallurgy*. 2022, vol. 65, no. 12, pp. 879–886. *https://doi.org/10.17073/0368-0797-2022-12-879-886*

Оригинальная статья

Деформация и разрушение Cr – Mn – C – N стали в литом состоянии

Е. Е. Дерюгин, Н. А. Наркевич, Ю. Ф. Гоморова

Институт физики прочности и материаловедения Сибирского отделения РАН (Россия, 634055, Томск, пр. Академический, 2/4)

Аннотация. Исследовано влияние граничных условий и скорости нагружения на деформационное поведение и разрушение стали на основе Cr – Mn – C – N аустенита в литом состоянии без дополнительной термической обработки. Закономерности деформации и разрушения стали проанализированы на основе данных испытаний на трехточечный изгиб образцов квадратного сечения с надрезом и без надреза, положенных ребром на опоры. Такое нетрадиционное расположение образца на опорах позволило обнаружить помимо начальной стадии упругой деформации стали еще две стадии развития деформации под действием внешней приложенной силы: стадию нелинейной деформации и стадию прерывистой деформации, предшествующей моменту разрушения образца. Показано, что с увеличением скорости нагружения сопротивление разрушению и протяженность стадии нелинейной деформации образца с надрезом увеличивается, а протяженность стадии прерывистой деформации уменьшается. Образец без надреза имеет продолжительную стадию нелинейной деформации и проявляет максимальную прочность при отсутствии стадии прерывистого течения. Завершение стадии нелинейной деформации соответствует моменту разрушения образца. Характерным свойством литой стали при заданных условиях нагружения является то, что разрушение образца совершается хрупко, несмотря на продолжительную стадию нелинейной деформации. Структурные металлографические и дифрактометрические исследования показали, что во всех испытаниях разрушение стали происходит хрупко без следов пластической деформации. Стадия нелинейной деформации стали определяется не дислокационной пластической деформацией, а механизмом $\gamma \rightarrow \alpha'$-превращения в аустенитных прослойках между нитридными и карбидными частицами под действием внешней приложенной силы. Стадия прерывистой деформации стали связана с процессом стабильного распространения трещины по поперечному сечению образца.

Ключевые слова: литая Cr – Mn – C – N сталь, дендритная структура, прерывистый распад, нитриды, испытания на изгиб, разрушение

© E. E. Deryugin, N. A. Narkevich, Yu. F. Gomorova, 2022

Финансирование: Работа выполнена в рамках государственного задания ИФПМ Сибирского отделения РАН (тема FWRW-2021-0009), а также при поддержке Российского научного фонда, грант № 22-29-00438.

Для цитирования: Дерюгин Е.Е., Наркевич Н.А., Гоморова Ю.Ф. Деформация и разрушение Cr – Mn – C – N стали в литом состоянии // Известия вузов. Черная металлургия. 2022. Т. 65. № 12. С. 879–886. https://doi.org/10.17073/0368-0797-2022-12-879-886

Introduction

Austenitic chromium-manganese steels with a high content of interstitial (C + N) elements possess high strain hardening [1 – 3], corrosion resistance [4, 5], and endurance under alternating loads [3, 6]. The presence of carbon in their composition not only simplifies melting (since it eliminates the need for oxygen blowing for carbon oxidation or the use of high-purity carbon-free charge components), but also improves strength properties. Works [7, 8] noted that nitrogen not only increases the strength, but, like manganese, increases the fluidity of steels, making them more technologically advanced than cast chromium-nickel steels.

Currently studies are being performed which are aimed at developing a method of making wear-resistant coatings from the steels under study [9 – 11], as well as composite coatings, in which Cr – Mn – C – N austenite is used as a matrix [12, 13].

Works [5, 7, 8] show that Cr – Mn – C – N steels have high strength properties, ductility and cold resistance, if nitrogen and carbon are dissolved in austenite. This is ensured by quenching from 1150 to 1200 °C in water and/or by strain hardening during cold strain, including frictional loads. Oil and natural gas production, storage and transportation systems require high-strength corrosion-resistant steels. Parts of complex shape can be made from these by casting only [8]. The Cr – Mn – C – N steels can be used as an alternative to expensive chromium-nickel steels. However, when slowly cooled from the liquid state or during isothermal aging in the temperature range from 400 to 950 ºC, the austenite in them decays with the formation of Me_2N and $Me_{23}C_6$ particles (where *Me* is metal) [5, 9]. Despite the fact that Cr_2N particles have a HCP (hexagonal closely packed) lattice and possess high hardness (according to different data from 15.7 [14] to 29.5 GPa [15]), aging has no positive effect on the strength properties of steels and reduces their ductility [16]. The composite structure[1] formed from interlaced strong dendritic axes and ductile interaxial sites provides high impact toughness of Cr8Mn28N cast steel.

The strain behaviour and fracture features of Cr – Mn – – C – N steel in the cast state, containing nitrides, carbonitrides and chromium carbides, as well as its crack resistance have not been studied.

The purpose of the present work is to study the influence of boundary conditions and the loading rate on the strain behavior and fracture resistance of cast Cr – Mn – C – N austenitic steel without additional heat treatment.

Material and research methods

Steel was melted under equilibrium conditions in a 50 kg induction furnace with a chromium-magnesite lining. Scrap metal, medium-carbon ferrochrome, ferromanganese and nitrogenous ferrochrome were used as a charge. Steel from the furnace was poured first into a ladle and then into five sand moulds. The sinkhead with a shrink hole was removed from the ingots obtained. The ingots of Cr – Mn – C – N steel under study did not contain gas holes. The chemical composition of the steel is given as follows, % (wt.): 24.40 Cr; 16.40 Mn; 1.10 Si; 0.18 Ni; 0.57 C; 0.70 N; 0.017 S; and the rest is Fe.

The structure was studied on an Axiovert 25 optical microscope (Zeiss, Germany) after etching in the C_2H_5OH, HCl and HNO_3 solution in the volume parts ratio of 3:2:1. The phase analysis was performed by *X*-ray diffractometry on XRD-7000 (Shimadzu, Japan) in CoK_α radiation. The structure of the fracture surface was studied on a scanning electron microscope (SEM) Tescan MIRA 3 LMU.

The strain behaviour of steel was studied under three-point bending of samples at room temperature on Instron 5582 testing machine (Instron, US) at vertical displacement rates of the crossarm of 0.30 and 0.01 mm/min according to the sample layouts on supports shown in Fig. 1. At least three samples of each material were tested.

Results and discussion

The steel under study has a high content of austenite-promoting elements. After quenching from 1100 °C this assured its position in the Schaeffler diagram [17] in the austenitic region (Fig. 2, point *1*). After casting into sand moulds the steel has dendritic structure (Fig. 3, *a*), in which, at high magnification, platy nitrides of Cr_2N can be observed. This corresponds to the equilibrium

[1] Gorobchenko S.L., Krivtsov Yu.S., Andreyev A.K., Solntsev Yu.P. Competitiveness of valves casting beyond impact strength or application of a new complex method for confirmation of reliability of austenitic steels for cryogenic valves. *Pipeline valves and equipment*. 2013. Electronic resource: http://www.valverus.info/popular/3219-konkurentosposobnost-armaturnogo-litya.html (access date: 04.08.2022).

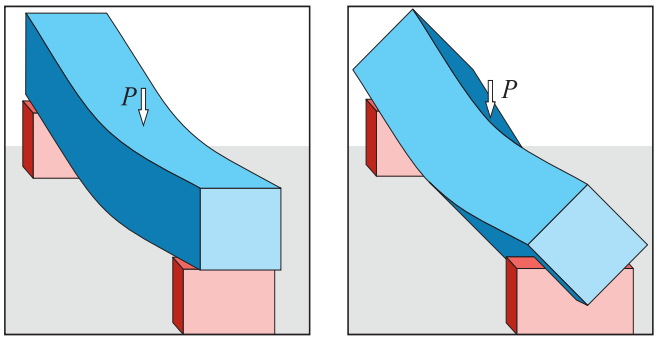

Fig. 1. Arrangement of the samples under three-point bending tests with support on the side of the sample (*a*) and on the edge of the sample (*b*)

Рис. 1. Расположение образцов при испытаниях на трехточечный изгиб с опорой на грань (*a*) и на ребро (*b*) образца

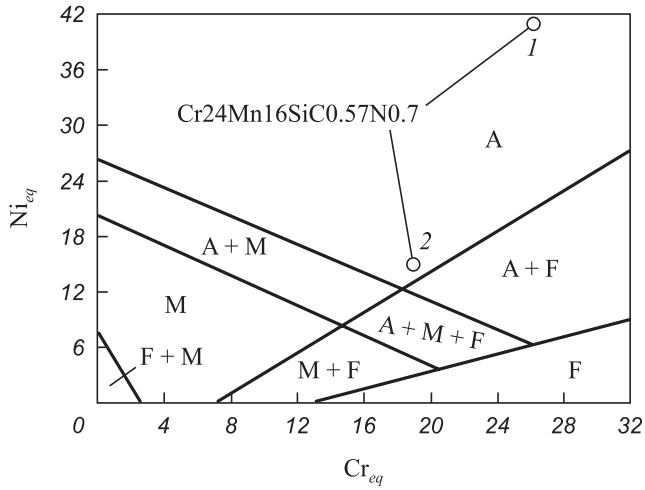

Fig. 2. Position of the steel under study in the Schaeffler diagram: *1* – after quenching from 1100 °C; *2* – in a cast (aged) state when austenite is depleted in chromium, carbon and nitrogen

Рис. 2. Положение рассматриваемой стали на диаграмме Шеффлера: *1* – после закалки от 1100 °C; *2* – в литом (состаренном) состоянии при обеднении аустенита хромом, углеродом и азотом

phase diagram for steel of similar composition, built on the basis of thermodynamic calculations [5].

Large (about 5 μm) individual chromium carbide particles present in the diagram [5] are differentiated well, around which intermittent decay of austenite is not observed in the chromium-depleted zones. The depletion of austenite with chromium, nitrogen and carbon reduces Ni_{eq} and Cr_{eq} (Ni_{eq} = Ni + 25N + 0.5Mn + 0.3Cu + 30C; Cr_{eq} = Cr + 2Si + 1.5Mo + 5V +1.75Nb +1.5Ti) and changes the steel position in the diagram without changing the phase (Fig. 2, point *2*).

The diffraction pattern (Fig. 3, *b*) shows reflections from the austenite planes. Reflections from particles are not detected in the diffraction pattern because of a very "noisy" background due to the dendritic structure.

Samples with the 5×5 mm cross-section with a shallow notch (0.5 mm deep, 0.3 mm wide) were loaded by the three-point bending method. In experiments with three-point bending, the beam is placed with a side on two supports, and force is applied to the center of the beam (Fig. 1, *a*) [18, 19]. In the present work, the beam was placed not with a side, but with a rib on supports (Fig. 1, *b*). It was assumed that such an arrangement would prolong the stage of plastic yield and stable crack propagation.

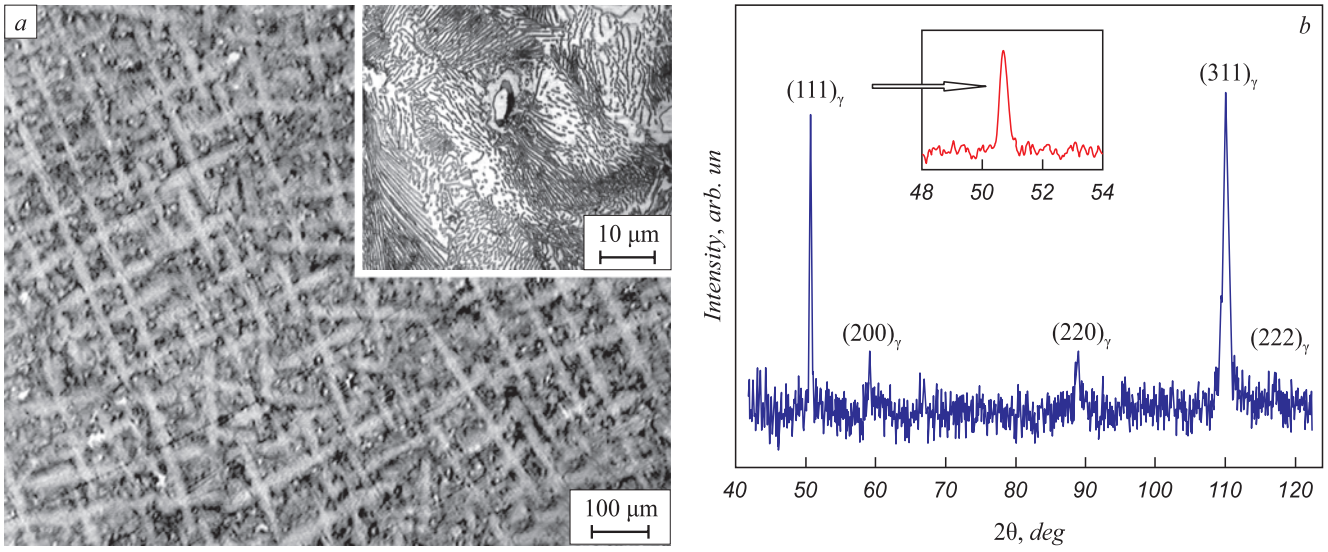

Fig. 3. Structure of cast Cr – Mn – C – N steel: *a* – metallographic pattern; *b* – X-ray diffraction pattern

Рис. 3. Структура литой Cr – Mn – C – N стали: *a* – металлографическое изображение; *b* – дифрактограмма

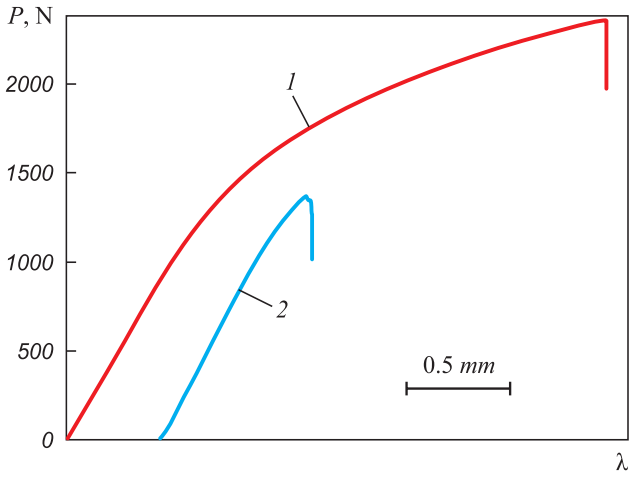

Fig. 4. Loading diagrams for Cr – Mn – C – N ssteel samples under three-point bending tests at a rate of v = 0.01 mm/min: *1* – with a notch; *2* – without a notch

Рис. 4. Диаграммы нагружения образцов Cr – Mn – C – N стали при испытаниях на трехточечный изгиб со скоростью 0,01 мм/мин: *1* – без надреза; *2* – с надрезом

Fig. 4 shows typical force P – bending λ diagrams of samples with the 5×5 mm cross-section, 50 mm long, when the distance between the supports L is 47 mm. Curve *1* refers to testing of a sample without a notch with slow loading rate of v = 0.01 mm/min. Steel fracture occurs at high external applied force (at P = 2355 ± 15 N). Two stages (stages *I* and *II* of elastic and nonlinear strain) are observed in diagram *1*. The nonlinear strain stage accounts for at least 60 % of the total strain of the sample. The beginning of the nonlinear strain stage is fixed at the external applied load of P_1 = 900 ± 6 N. The end of the nonlinear strain stage corresponds to the moment of sample failure. Thus, a characteristic property of cast steel under the given loading conditions is that the fracture of the sample is brittle, despite the prolonged stage of nonlinear strain.

Curve *2* is an example of strain of the sample with a notch in the center of the rib. The notch significantly reduces the strength of the sample and decreases the nonlinear strain stage, which in this case does not exceed 11 % of the sample total strain. The deviation from the elastic strain stage is fixed at a lower value of force (P_1 = 813 N). In addition, from the moment the maximum load of P_{max} = 1360 N is reached, there is no fracture of the sample and stage *III* is observed, at which relaxation of the external applied force up to 1220 N occurs in an intermittent manner. The irregular nature of external load relaxation testifies to the process of slip-stick propagation of the main crack across the sample. Fig. 5 shows the moment of the main crack development from the notch registered at stage *III* of the sample strain.

The effect of the loading rate on strain of the samples with a notch is shown in Fig. 6. Curve *1* corresponds to the rate of v = 0.3 mm/min and curve *2* corresponds to the rate of v = 0.01 mm/min. The comparison shows that the qualitative appearance of the diagrams does not change in this case. In both cases, three stages of strain (elastic, nonlinear and discontinuous strain) can be observed. However, as the loading rate increases, the strength of the material increases significantly.

With a low (v = 0.01 mm/min) strain rate of the sample, the maximum load is 1360 N, while with v = 0.3 mm/min it reaches a level of 1567 N. The transition to the nonlinear strain stage is almost independent of the loading rate of the sample and is fixed at a level of P_1 = 800 ± 10 N.

An increase in the loading rate is accompanied by an increase in the stage of discontinuous strain associated with the relaxation of the external applied force. In the case of high (v = 0.3 mm/min) loading rate (Fig. 5, curve *2*) there is even a decrease in force by the value of ΔP = 138 N.

Curve *3* in Fig. 6 corresponds to the strain at a rate of v = 0.01 mm/min of a sample with a chevron notch, placed on supports not with a rib but with a side. The sample has the lowest mechanical indicators (P_{max} = 891 N; P_1 = 670 N; ΔP = 15 N; nonlinear strain less than 1 %).

The analysis of fracture surfaces of Cr – Mn – C – N steel showed that the fracture character of all samples was

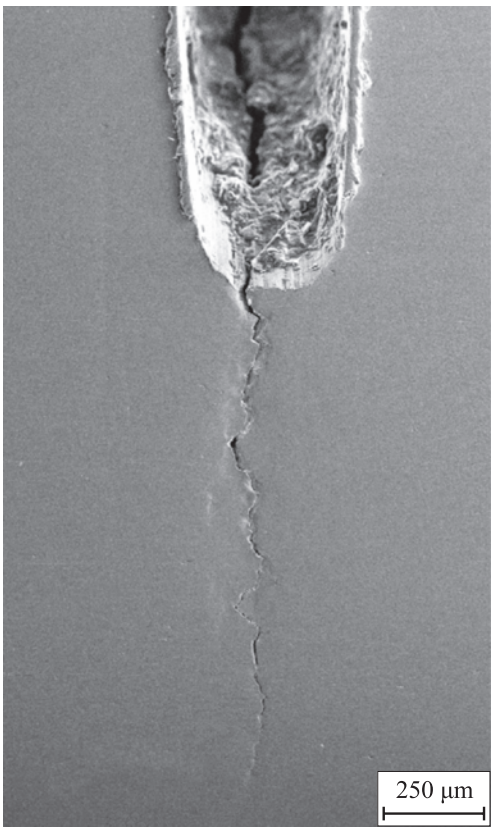

Fig. 5. Propagation of a crack from a notch

Рис. 5. Распространение трещины от надреза

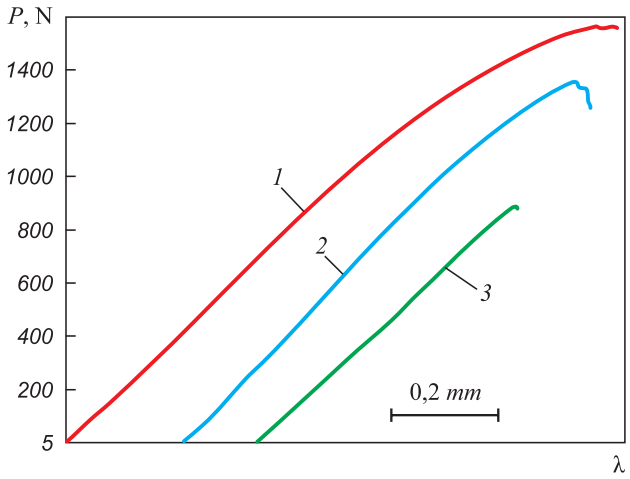

Fig. 6. Loading diagrams of Cr – Mn – C – N steel samples with a notch under three-point bending tests at a strain rate of 0.3 mm/min (*1*), 0.01 mm/min (*2*) and sample with a chevron notch at a rate of 0.3 mm/min (*3*)

Рис. 6. Диаграммы нагружения образцов Cr – Mn – C – N стали с надрезом при испытаниях на трехточечный изгиб со скоростью деформации 0,3 мм/мин (*1*), 0,01 мм/мин (*2*) и образца с шевронным надрезом со скоростью 0,3 мм/мин (*3*)

brittle with morphological features in the form of foliation (Fig. 7, *a*) due to the steel structure with platy dispersed particles of Cr_2N (Fig. 3, *a*). Nitrides Cr_2N decompose in the process of loading, provoking failure of the sample as a whole. In this regard, there is qualitative similarity between the metallographic image of the structure (Fig. 3, *a*) and the fracture surface of the steel in question (Fig. 7, *a*). This still allows for the possibility that an insignificant fraction of nonlinear strain of the sample is due to plastic yield of austenite. On the diffraction pattern obtained from the fracture surface, in addition to reflections from the austenite planes, there is a reflection from plane (110) of α′-martensite with BCC lattice (Fig. 7, *b*).

The change in the phase composition during three-point bending tests can be estimated from temperature *Md*30 [20], at which the structure consists of 50 % γ-phase and 50 % α'-martensite after 30 % strain. Since only a part of the (C + N) content remains in solid solution when the casting is cooled, and the rest is in bound form in chromium nitrides and carbides (Fig. 2, point *2*). The calculated *Md*30 temperature of steel in the quenched state and austenite in the aged state increases to –18 °C. The strain of steel at room temperature initiates the γ → α′-transformation in austenitic interlayers between the nitride and carbide particles (Fig. 7, *b*). The strain process is also evidenced by an increase in the half-widths of the diffraction maxima in the diffraction pattern obtained from the steel fracture, when compared to the diffraction pattern obtained from the original cast steel structure (Fig. 3, *b*; Fig. 5, *b*). Respectively, the bulk of the nonlinear strain of steel is provided not by the plastic yield of the austenite, but by γ → α′-transformation under the effect of an external applied force.

In order to stimulate the TRIP effect, a sufficiently high local stress σ_{TRIP} is required. By definition this is less than the stress of the onset of local fracture of material σ_{TRIP}. Nonlinear strain from the TRIP effect depends on the efficiency of the stress concentrator. In the sample with a chevron notch placed on supports with a side, high stress concentration occurs in small vicinity of the chevron under the effect of an external force. Therefore, the contribution of γ → α′-transformation to the inelastic strain by the time the sample fails will be minimum (Fig. 6, curve *3*).

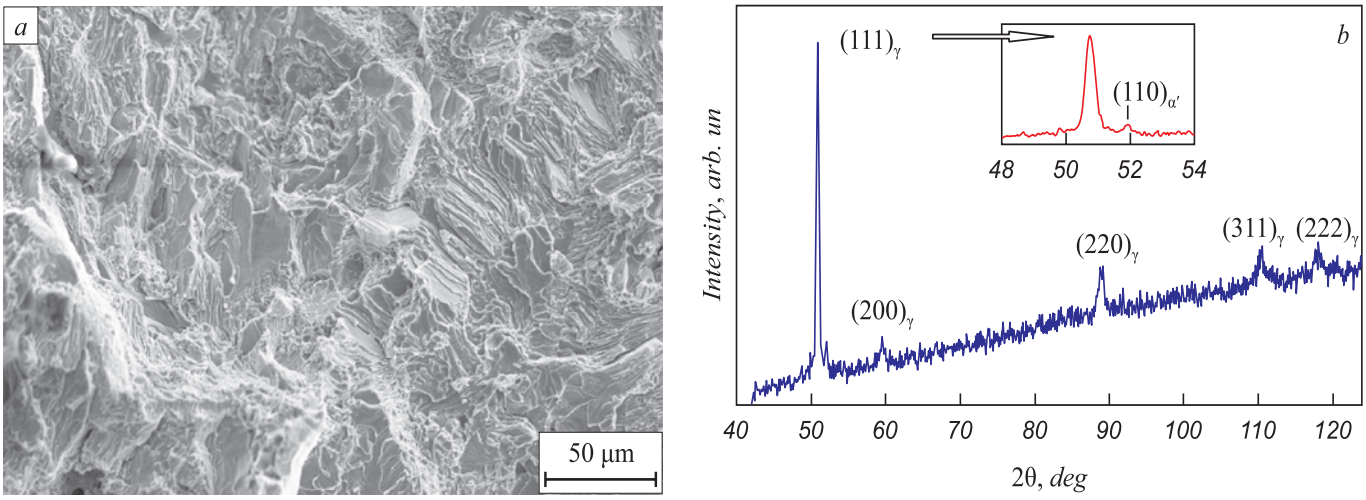

Fig. 7. Structure of the fracture surface of cast Cr – Mn – C – N steel: *a* – SEM pattern; *b* – *X*-ray diffraction pattern

Рис. 7. Структура поверхности разрушения литой Cr – Mn – C – N стали: *a* – РЭМ изображение; *b* – дифрактограмма

In contrast, a wide region of increased stresses is observed when the sample without a notch is loaded, placed with a rib on supports. Reaching the σ_{TRIP} value in the wide region is only possible if the external applied stress is high enough. During the loading process, a quite large volume of material will be covered by the $\gamma \rightarrow \alpha'$-transformation before fracture begins. The onset of fracture will correspond to the maximum external applied force P_{max} and the contribution of $\gamma \rightarrow \alpha'$-transformation to the inelastic strain of the sample will also be maximum.

The $\gamma \rightarrow \alpha'$-transformation process is always accompanied by stress relaxation. Therefore, slow loading will involve a larger volume of the sample in the phase transformation compared to fast loading. This explains the quantitative and qualitative difference between loading diagrams *1* and *2* (Fig. 6).

Material fracture at the final stage of loading is determined by the rate of release of elastic energy during crack propagation. The more the elastic energy accumulated in the sample volume, the lower the probability of stable crack propagation at the prefracture stage. Respectively, the higher the maximum of applied force P_{max} by the end of the nonlinear strain stage, the greater the crack length in the sample section, and therefore the longer the development of stage *III* of strain. The value of P_{max} = 2355 N when testing the sample without a concentrator with the loading rate of 0.01 mm/min is so high that the sample fails spontaneously (Fig. 4, diagram *1*).

Conclusion

The paper studies the strain and fracture behavior of austenitic Cr–Mn–C–N steel in the cast state on the basis of three-point bending test data of square-section samples, placed with a rib on supports. Such arrangement of the sample on supports revealed new regularities that cannot be detected under standard test conditions when the sample is placed with a side on supports.

The study clearly revealed three stages of steel strain under the effect of an external applied force (stage *I* of elastic strain, stage *II* of nonlinear strain and stage *III* of discontinuous strain preceding the moment of sample failure).

It was demonstrated that as the loading rate increases, the fracture resistance and the extent of the nonlinear strain stage of the sample with a notch increases, and the extent of the discontinuous strain stage decreases.

The sample without a notch exhibits maximum strength in the absence of the discontinuous strain stage.

The studies showed that the discontinuous character of the loading diagram is associated with the process of steady crack propagation across the sample. In all cases, the steel fracture is brittle without traces of plastic yield. The analysis of the results obtained shows that the nonlinear strain stage of steel is determined not by dislocation plastic yield, but by the mechanism of $\gamma \rightarrow \alpha'$ transformation in austenitic interlayers between nitride and carbide particles under the effect of an external applied force.

References / Список литературы

1. Berns H., Gavriljuk V., Riedner S., Tyshchenko A. High strength stainless austenitic CrMnCN stees. Part I: Alloy design and properties. *Steel Research International*. 2007, vol. 78, no. 9, pp. 714–719. https://doi.org/10.1002/srin.200706274
2. Gavriljuk V., Razumov O., Petrov Y., Surzhenko I., Berns H. High strength stainless austenitic CrMnCN stees. Part II: Structural changes by repeated impacts. *Steel Research International*. 2007, vol. 78, no. 9, pp. 720–723. https://doi.org/10.1002/srin.200706275
3. Schymura M., Fischer A. Fatigue of austenitic high interstitial steels – The role of N and C. *Advanced Materials Research*. 2014, vol. 891-892, pp. 403–409. https://doi.org/10.4028/www.scientific.net/AMR.891-892.403
4. Berezovskaya V., Merkushkin E.A. Structure and phase transformations in high nitrogen and high interstitial steels of different alloying systems – Short Review. *Defect and Diffusion Forum*. 2021, vol. 410, pp. 167–172. https://doi.org/10.4028/www.scientific.net/DDF.410.167
5. Niederhofer P., Siebert S., Huth S., Theisen W., Berns H. High interstitial FeCrMnCN austenitic stainless steels for use in tribocorrosive environments. In: *Proceedings of the 12th Int. Conf. on High Nitrogen Steels (HNS),* Hamburg, 2014, pp. 50–57.
6. Schymura M., Stegemann R. Crack propagation behavior of solution annealed austenitic high interstitial steels. *International Journal of Fatigue*. 2015, vol. 79, no. 10, pp. 25–35. https://doi.org/10.1016/j.ijfatigue.2015.04.014
7. Solntsev Yu.R. *Cold-Resistant Steels and Alloys*. St. Petersburg: Khimizdat, 2005, 476 p. (In Russ.).

1. Berns H., Gavriljuk V., Riedner S., Tyshchenko A. High strength stainless austenitic CrMnCN stees. Part I: Alloy design and properties // Steel Research International. 2007. Vol. 78. No. 9. P. 714–719. https://doi.org/10.1002/srin.200706274
2. Gavriljuk V., Razumov O., Petrov Y., Surzhenko I., Berns H. High strength stainless austenitic CrMnCN stees. Part II: Structural changes by repeated impacts // Steel Research International. 2007. Vol. 78. No. 9. P. 720–723. https://doi.org/10.1002/srin.200706275
3. Schymura M., Fischer A. Fatigue of austenitic high interstitial steels – The Role of N and C // Advanced Materials Research. 2014. Vol. 891-892. P. 403–409. https://doi.org/10.4028/www.scientific.net/AMR.891-892.403
4. Berezovskaya V., Merkushkin E.A. Structure and phase transformations in high nitrogen and high interstitial steels of different alloying systems – Short Review // Defect and Diffusion Forum. 2021. Vol. 410. P. 167–172. https://doi.org/10.4028/www.scientific.net/DDF.410.167
5. Niederhofer P., Siebert S., Huth S., Theisen W., Berns H. High interstitial FeCrMnCN austenitic stainless steels for use in tribocorrosive environments. In: Proceedings of the 12th Int. Conf. on High Nitrogen Steels (HNS). Hamburg, 2014. P. 50–57.
6. Schymura M., Stegemann R. Crack propagation behavior of solution annealed austenitic high interstitial steels // International Journal of Fatigue. 2015. Vol. 79. No.10. P. 25–35. https://doi.org/10.1016/j.ijfatigue.2015.04.014
7. Солнцев Ю.Р. Хладостойкие стали и сплавы. Санкт-Петербург: Химиздат. 2005. 476 с.

8. Kostina M.V., Polomoshnov P.Yu., Blinov V.M., Muradyan S.O., Kostina V.S. Cold resistance of new casting Cr – Mn – Ni – Mo – N steel with 0.5 % of N. Part 1. *Izvestiya. Ferrous Metallurgy*. 2019, vol. 62, no. 11, pp. 894–906. (In Russ.). https://doi.org/10.17073/0368-0797-2019-11-894-906
9. Panin V.E., Narkevich N.A., Durakov V.G., Shulepov I.A. Control of the structure and wear resistance of a carbon-nitrogen austenitic steel coating produced by electron beam cladding. *Physical Mesomechanics*. 2021, vol. 24, no. 1, pp. 53–60. https://doi.org/10.1134/S1029959921010082
10. Tagil'tseva D.N., Narkevich N.A., Shulepov I.A., Moiseenko D.D. Relaxation capacity and cracking resistance of nitrous coating produced by electron-beam facing of 0.6C-24Cr-0.7N-16Mn steel powder during wear by hard abrasive under heavy loads. *Journal of Friction and Wear*. 2014, vol. 35, no. 2, pp. 104–110. https://doi.org/10.3103/S1068366614020159
11. Narkevich N.A., Tagil'tseva D.N., Durakov V.G., Shulepov I.A., Ivanova E.A. Structure and wear resistance of electron-beam nitrous coatings. *Journal of Friction and Wear*. 2012, vol. 33, no. 5, pp. 374–380. https://doi.org/10.3103/S106836661205008X
12. Ivanova E.A., Narkevich N.A. Structure and wear resistance of nitrogenous dispersed coatings reinforced with nitrated ferrovanadium obtained by electron-beam surfacing. *Izvestiya. Ferrous Metallurgy*. 2008, vol. 51, no. 10, pp. 41–44. (In Russ.).
13. Narkevich N.A., Tagil'tseva D.N., Durakov V.G., Shulepov A.I., Smirnov A.I. Structure and tribological and mechanical properties of nitrogen electron-beam coatings dispersion-hardened by V(C, N) particles. *Physics of Metals and Metallography*. 2013, vol. 114, no. 6, pp. 535–544. https://doi.org/10.1134/S0031918X13060100
14. Tu J.-N., Duh J.-G., Tsai S.-Yu. Morphology, mechanical properties, and oxidation behavior of reactively sputtered Cr–N films. *Surface and Coatings Technology*. 2000, vol. 133-134, no. 2-3, pp. 181–185. https://doi.org/10.1016/S0257-8972(00)00961-0
15. Pakala M, Lin R.Y. Reactive sputter deposition of chromium nitride coatings. *Surface and Coatings Technology*. 1996, vol. 81, no. 2-3, pp. 233–239. https://doi.org/10.1016/0257-8972(95)02488-3
16. Simmons J.W. Overview: High-nitrogen alloying of stainless steels. *Materials Science and Engineering: A*. 1996, vol. 207, no. 2, pp. 159–169. https://doi.org/10.1016/0921-5093(95)09991-3
17. Colombier L., Hochmann J. *Stainless and Heat Resisting Steels*. Hodder Arnold H&S, 1976, 560 p.
18. Paimushin V.N., Tarlakovskii D.V., Kholmogorov S.A. On non-classical form of stability loss and destruction of composite test samples under three-point bending. *Uchenye zapiski. Kazan. un-ta. Ser. Fiz.-matem. nauki*. 2016, vol. 158, no. 3, pp. 350–375. (In Russ.).
19. *GOST R 56805 – 2015 (ISO 14125:1998). Polymer composites. Methods for determining mechanical characteristics during bending*. Moscow: Standartinform, 2016. (In Russ.).
20. Pickering F.B. *Physical Metallurgy and the Design of Steels*. London: Applied Science Publisher Ltd., 1978, 275 p.

8. Костина М.В., Поломошнов П.Ю., Блинов В.М., Мурадян С.О., Костина В.С. Хладостойкость новой литейной Cr – Mn – Ni – – Mo – N стали с 0,5 % N. Часть 1 // Известия вузов. Черная металлургия. 2019. Т. 62. № 11. С. 894–906. https://doi.org/10.17073/0368-0797-2019-11-894-906
9. Панин В.Е., Наркевич Н.А., Дураков В.Г., Шулепов И.А. Управление структурой и износостойкостью электроннолучевого покрытия из углеродоазотистой аустенитной стали // Физическая мезомеханика. 2020. Т. 23. № 2. С. 15–23. https://doi.org/10.24411/1683-805X-2020-12002
10. Тагильцева Д.Н., Наркевич Н.А., Шулепов И.А., Моисеенко Д.Д. Релаксационная способность и трещиностойкость азотистого покрытия, полученного электронно-лучевой наплавкой порошка стали 60Х24АГ16 при высоконагруженном изнашивании твердым абразивом // Трение и износ. 2014. Т. 35. № 2. С. 142–150.
11. Наркевич Н.А., Тагильцева Д.Н., Дураков В.Г., Шулепов И.А., Иванова Е.А. Структура и износостойкость электронно-лучевых азотистых покрытий // Трение и износ. 2012. Т. 33. № 5. С. 512–520.
12. Иванова Е.А., Наркевич Н.А. Структура и износостойкость азотистых дисперсноупрочненных азотитрованным феррованадием покрытий, полученных электронно-лучевой наплавкой // Известия вузов. Черная металлургия. 2008. Т. 51. № 10. С. 41–44.
13. Наркевич Н.А., Тагильцева Д.Н., Дураков В.Г., Шулепов А.И., Смирнов А.И. Структура, трибологические и механические свойства азотистых электронно-лучевых покрытий, дисперсноупрочненных частицами V(C, N) // Физика металлов и металловедение. 2013. Т. 114. № 6. С. 583–592. https://doi.org/10.7868/S0015323013060107
14. Tu J.-N., Duh J.-G., Tsai S.-Yu. Morphology, mechanical properties, and oxidation behavior of reactively sputtered Cr–N films // Surface and Coatings Technology. 2000. Vol. 133-134. No. 2-3. P. 181–185. https://doi.org/10.1016/S0257-8972(00)00961-0
15. Pakala M, Lin R.Y. Reactive sputter deposition of chromium nitride coatings // Surface and Coatings Technology. 1996. Vol. 81. No. 2-3. P. 233–239. https://doi.org/10.1016/0257-8972(95)02488-3
16. Simmons J.W. Overview: High-nitrogen alloying of stainless steels // Materials Science and Engineering: A. 1996. Vol. 207. No. 2. P. 159–169. https://doi.org/10.1016/0921-5093(95)09991-3
17. Colombier L., Hochmann J. Stainless and Heat Resisting Steels. Hodder Arnold H&S, 1976. 560 p.
18. Паймушин В.Н., Тарлаковский Д.В., Холмогоров С.А. О неклассической форме потери устойчивости и разрушении композитных тест-образцов в условиях трехточечного изгиба // Ученые записки. Казан. ун-та. Сер. Физ.-матем. науки. 2016. Т. 158. № 3. С. 350–375.
19. ГОСТ Р 56805-2015 (ИСО 14125:1998). Композиты полимерные. Методы определения механических характеристик при изгибе. Москва: Стандартинформ. 2016.
20. Pickering F.B. Physical Metallurgy and the Design of Steels. London: Applied Science Publisher Ltd., 1978. 275 p.

Information about the Authors / Сведения об авторах

Evgenii E. Deryugin, *Dr. Sci. (Phys.–Math.), Prof., Leading Researcher,* Institute of Strength Physics and Materials Science, Siberian Branch of Russian Academy of Sciences
ORCID: 0000-0003-2195-4906
E-mail: dee@ispms.tsc.ru

Natal'ya A. Narkevich, *Cand. Sci. (Eng.), Assist. Prof., Senior Researcher,* Institute of Strength Physics and Materials Science, Siberian Branch of Russian Academy of Sciences
ORCID: 0000-0001-5179-1955
E-mail: natnark@list.ru

Евгений Евгеньевич Дерюгин, *д.ф.-м.н., профессор, ведущий научный сотрудник,* Институт физики прочности и материаловедения Сибирского отделения РАН
ORCID: 0000-0003-2195-4906
E-mail: dee@ispms.tsc.ru

Наталья Аркадьевна Наркевич, *к.т.н., доцент, старший научный сотрудник,* Институт физики прочности и материаловедения Сибирского отделения РАН
ORCID: 0000-0001-5179-1955
E-mail: natnark@list.ru

Yulia F. Gomorova, *Cand. Sci. (Eng.), Research Associate,* Institute of Strength Physics and Materials Science, Siberian Branch of Russian Academy of Sciences
ORCID: 0000-0002-0880-2898
E-mail: gomjf@ispms.ru

Юлия Федоровна Гоморова, *к.т.н., научный сотрудник,* Институт физики прочности и материаловедения Сибирского отделения РАН
ORCID: 0000-0002-0880-2898
E-mail: gomjf@ispms.ru

Contribution of the Authors

E. E. Deryugin – formation of the main idea, substantiation of the topic relevance, elaboration of the content of main sections, conducting the three-point bending test, final editing, preparation of the conclusions.
N. A. Narkevich – structure research, X-ray diffraction analysis, selection of the references.
Yu. F. Gomorova – preparation of samples for testing, electron microscopic analysis of the destruction surface of Cr – Mn – C – N steel.

Вклад авторов

Е. Е. Дерюгин – создание идеи статьи, обоснование актуальности темы, проработка содержания основных разделов, испытания на трехточечный изгиб, окончательная правка, подготовка заключения.
Н. А. Наркевич – исследование структуры, рентгеноструктурный анализ, подбор библиографических ссылок.
Ю. Ф. Гоморова – подготовка образцов к испытаниям, электронно-микроскопические исследования поверхности разрушения Cr – Mn – C – N стали.

Received 04.08.2022
Revised 22.08.2022
Accepted 05.09.2022

Поступила в редакцию 04.08.2022
После доработки 22.08.2022
Принята к публикации 05.09.2022